

Lifetime Maximization in UWB Sensor Networks for Event Detection

Ghasem Naddafzadeh Shirazi, *Student Member, IEEE*, and Lutz Lampe, *Senior Member, IEEE*

Abstract—The operational lifetime of a wireless sensor network (WSN) for event detection is determined by the maximum time that the network is able to meet given detection requirements (DRs), i.e., the probabilities of detection and false alarm demanded by the application. In this paper, we address the problem maximizing lifetime of such WSNs through optimizing quantization and routing of event measurements. In particular, we consider the task of monitoring multiple events and reporting the observations to a sink, whereby sensor nodes adapt their data generation rate and the data flow distribution in the network for the purpose of lifetime maximization. We make use of ultra-wideband (UWB) signaling at the physical layer, which is well-suited for event-detection WSNs, because of the low-energy consumption for data transmission and relative robustness to multi-user interference. Expressing the DRs as convex constraints in the optimization variables, we present a convex-optimization framework for lifetime maximization of event detection UWB-based WSNs. Furthermore, based on the dual decomposition approach, we propose a decentralized algorithm, which makes it possible to solve the lifetime-maximization problem in a distributed manner and thus shares the computational complexity among network nodes and is robust to artifacts like node failures. Numerical results show that the proposed joint adaptation of quantization and routing leads to significant improvements in network operational lifetime compared to benchmark approaches known from literature.

Index Terms—Lifetime maximization problem, Event detection wireless sensor networks, Convex optimization, Distributed optimization.

I. INTRODUCTION

Wireless sensor networks (WSNs) are being considered and used in a wide range of applications such as event detection, target tracking, home automation, etc. Since the sensor nodes operate on small batteries with limited energy and it is usually impossible to provide external sources of energy, minimization of energy consumed for data communication, while still meeting the functionality requirements, is an important challenge in WSNs [1]. Preservation of energy for communication can be achieved through optimization of different parameters, such as sleep frequency [2], [3], transmission energy [4], data flows and bit rates [5], and node density (prior to node deployment) [6].

In this paper, we consider a specific class of WSNs, namely WSNs used for event detection, in which the sensor nodes observe the status of one or more events at known locations and report their observations (measurements) to a fusion center (sink) through multihop routing. At the sink, a decision about the event status is made using the received measurement results from reporting sensors. There are numerous applications for this type of WSNs, for example in radar, sonar and ultrasound surveillance systems [7], [8], for disaster monitoring and emergency response [9], habitat monitoring [10], and for patient

monitoring in health-care facilities [11]. We aim at optimizing the routing of measurement data from nodes to the sink such as to maximize the operational lifetime of the WSN. Here, the operational lifetime is defined as the time from the beginning of operation of the WSN until the WSN is unable to perform its task, i.e., until given detection requirements (DRs) cannot be met anymore.

Despite many existing studies on the general lifetime problem, e.g. [2], [4], [6], [12]–[15], energy efficient routing strategies specific to event detection WSNs have not been investigated in the literature until recently [7], [8]. Yang *et al.* [7] consider active radar-like sensors responsible for detecting the presence of an object, and use the Neyman-Pearson hypothesis test [16], [17] to design their decision variables. They investigate minimum energy routing with guaranteed DRs (MERG), and use a Lagrangian relaxation technique to maximize a lower bound for lifetime. Li and AlRegib [8] consider the maximization of the lifetime upper-bound (MLB) as a function of the number of bits used at a node for representing its measurements. This enables nodes to tradeoff accuracy of the reported measurement with energy consumption for communication. Their approach is based on decoupling the problem of quantization from the routing problem. Specifically, each node first minimizes a local cost function to decide on the number of bits that it will generate for detecting an event. Then a linear program is solved to obtain the optimal routes and flows of the entire network. The decoupling significantly decreases the complexity of the problem.

The algorithms proposed in [7] and [8] provide useful solutions for the energy efficiency problem under event detection requirements. In this paper we strive to improve these works by considering a more general framework as well as providing more effective techniques for maximizing the lifetime. Specifically, we consider and maximize *exact* network lifetime subject to DRs, compared to the optimization of lower and upper bounds on lifetime in [7] and [8]. We also improve upon [7] by considering variable generation rates and balancing them based on the sensor's location and available energy. In addition, we overcome the well-known *bottleneck node* problem, i.e., fast depletion of a node with a higher amount of flow compared to other nodes, by jointly optimizing the routes for all event locations, such that the flows can be balanced among different paths to prolong lifetime. This approach is similar to methods that consider multi-commodity flows in the network [14], [15]. However, in our framework routing parameters are jointly optimized with generation rates and considering DRs. An alternative approach for optimizing the network lifetime is to reduce the number of communicated bits by the help of data aggregation, e.g. [5], [18]. In data aggregation, each sensor merges the received data from other sensors with its local measurements according to the correlation between them. Note that, however, in our problem generation rates are jointly optimized with the routing parameters and thus performing data aggregation is unnecessary. This also simplifies the structure of sensors since they are exempted from decoding, processing, and merging the received data.

For the physical layer of the WSN devices, we consider the use of impulse radio (IR) ultra-wideband (UWB) transmission for its low energy consumption and simple and cost-effective radios [19]–[22].

Copyright (c) 2011 IEEE. Personal use of this material is permitted. However, permission to use this material for any other purposes must be obtained from the IEEE by sending a request to pubs-permissions@ieee.org.

This work was supported by the National Sciences and Engineering Research Council (NSERC) of Canada under Grant STPGP 364995. Part of this work has been presented at the 2010 IEEE International Conference on Communications (ICC), South Africa. The authors are with the Department of Electrical and Computer Engineering, University of British Columbia, Vancouver, BC, Canada, V6T 1Z4 (e-mail: {naddaf, lampe}@ece.ubc.ca). The authors would like to thank anonymous reviewers for their valuable comments and their help to improve the quality of the paper.

UWB pulses are transmitted in a short duration of time, on the order of a few nanoseconds, using time hopping (TH) codes. Different nodes transmit using different TH code sequences, providing UWB with the advantage of accommodating concurrent transmissions. Moreover, interference mitigation methods [23] remove the need for exclusive transmission regions. Thus, it is not required to employ carrier sensing or other complicated medium access control protocols provided that the interference is balanced among multiple routes [24]. All of these properties make UWB radio an excellent choice for sensor networks in which energy efficiency and simplicity is highly desirable. High data rates are also achievable using UWB radio due to the large available bandwidth. In this regard, we will make use of the fact that the UWB link capacity can well be approximated as a linear function of signal to interference and noise ratio (SINR) due to the very low transmission power [25].

There are a number of related literatures on UWB based WSN for event detection. For example, in a recent work, Bai *et al.* [26] propose and compare the performance of different distributed detection techniques in UWB sensor networks under energy constraints. However, only the UWB physical layer is considered in this study and routing layer optimization is left unhandled. Xu *et al.* [27] provide some upper bounds on the operational lifetime of a general UWB sensor network, and Shi and Hou [28] investigate the UWB sensor network maximum rate feasibility problem (URFP). They solve this non-linear problem using a linearization relaxation technique and devise a heuristic for connecting the source nodes to the sink. None of these works consider the exact lifetime maximization of sensor networks for a given detection requirement.

Direct formulation of lifetime maximization commonly leads to a centralized optimization problem [13], [15]. In order to convert the centralized optimization into smaller distributed sub-problems, decomposition techniques can be used. For example, Madan and Lall [14] decompose the standard lifetime maximization problem using the dual function and Lagrange multipliers on the energy and flow constraints. In the distributed methods, nodes are required to exchange the Lagrange multipliers and local flow and lifetime parameters with their neighbors and update them iteratively until converging to the near-optimal solution. In order to make the dual function differentiable, regularization techniques are sometimes applied to the objectives. For example, [29] further changes the objective to optimize a weighted sum of lifetime and routing cost. In this paper, we apply this distributed optimization framework to the problem at hand and extend it to also take into account the DRs.

In summary, we address the problem of lifetime maximization in UWB based sensor networks for event detection. Our method jointly optimizes routes to detect multiple events, which avoids the overuse of individual sensor nodes in multiple paths known to decrease operational lifetime. Furthermore, nodes send their measurements with different precisions to the sink. For example, a node with a larger/smaller amount of remaining energy represents its measurement with larger/smaller number of bits. By considering this degree of freedom in our model, nodes can easily trade off accuracy with energy consumption, leading to an overall increase in network lifetime. The optimization problem is formulated as a convex program, and numerical results for selected network examples show that the lifetime achieved with this program are considerably increased compared to those obtained with the routing schemes proposed in [7], [8], [28]. A distributed method is also proposed as a solution that shares the computational load for optimization among sensors and only requires local communication.

The remainder of this paper is organized as follows. System model and assumptions made are described in detail in Section II. The optimization framework for UWB-based sensor network lifetime

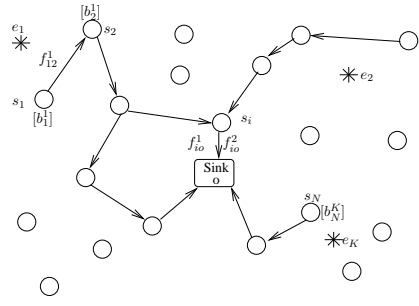


Fig. 1. Illustration of the UWB-based sensor network for event detection. N UWB-enabled nodes (circles, s_i , $i = 1, \dots, N$) are located around a sink (square, o). They measure data from K events (stars, e_k , $k = 1, \dots, K$), quantize the measurements into b_i^k bits, and report it to the sink, where f_{ij}^k denotes the data flow from s_i to s_j for reporting the event e_k .

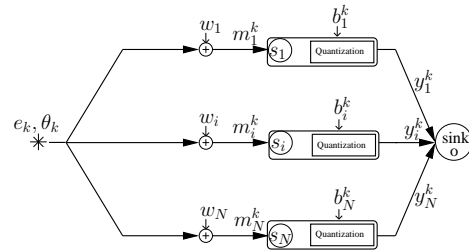


Fig. 2. Sensing model under presence of e_k .

maximization is presented in Section III, and its distributed version is explained in Section IV. The performance of the proposed method is evaluated and compared by means of simulations in Section V. Finally, Section VI concludes this paper.

II. SYSTEM MODEL

We consider a multiple-event detection UWB-based sensor network, as illustrated in Figure 1. In this network, N sensors s_i , $i = 1, \dots, N$, should sense the K events e_k , $k = 1, \dots, K$, and report their measurements to the sink. The sensors s_i are placed at locations (x_i, y_i) , and events e_k are expected to occur at locations (x'_k, y'_k) . Let d_{ij} denote the Euclidean distance between s_i and s_j . Each node s_i can transmit to or receive from the nodes in its communication range D , i.e., its neighbors $\mathcal{N}_i = \{s_j : d_{ij} \leq D\}$. Details about the sensing model are provided in Section II-A. After sensing the events, the measured data is routed to the sink via multipath routing as explained in Section II-C. Energy consumption at the nodes for data transmission and data flow in the links are determined by the UWB-specific transmission and link capacity models, as will be described in Section II-B.

A. Sensing Model

Consider the task of sensing in the network for gathering information about a possible event at a given location. Figure 2 illustrates the sensing model for an event e_k in such a network. The presence of the event e_k is indicated by the parameter θ_k , which is observed by the sensors. Let H_1^k and H_0^k , $k = 1, \dots, K$, indicate the presence and absence of e_k , respectively. Under this model, the measured signal at sensor s_i is given by

$$m_i^k = \begin{cases} w_i, & H_0^k, \\ \theta_k + w_i, & H_1^k, \end{cases} \quad (1)$$

where w_i is Gaussian measurement noise with variance σ_i^2 . We assume that the events occur at locations which are far from each

other relative to the communication range D . Therefore, in (1) it is implied that each sensor observes at most one event (cf. also [11], [30]). Furthermore, note that known attenuation of observations can be easily handled by the sensing model in (1). Specifically, denoting the attenuation between s_i and e_k by a_i^k , the model

$$m_i^k = a_i^k \theta_k + w_i' \quad (2)$$

with noise variance $\sigma_i'^2$ reduces to (1) by letting $m_i^k = m_i^k/a_i^k$ and $\sigma_i^2 = \sigma_i'^2/(a_i^k)^2$ [8], [31]. We would also like to point out that (1) includes the active sensing framework of [7] as a special case, where sensors should send signals to the location of e_k with the sensing energy E_s and measure the reflected signal. In fact, (2) can be specified to the active sensing model by applying the deterministic value $\theta_k = \sqrt{E_s}$ and setting $a_i^k = \sqrt{\beta_{ik}}$, where β_{ik} is the path loss coefficient between e_k and s_i . Note, however, that in the general model (1) the value of θ_k is unknown, and the sensors are required to estimate it when e_k is present (H_1^k).

We further assume that the measurement m_i^k is quantized into $b_i^k \in \{1, 2, \dots, b_{\max}\}$ bits, i.e., s_i sends only b_i^k bits for the measurement m_i^k to the sink. The quantization interval, $\mathcal{M}_R = [-M, M]$, with a fixed known $M > 0$ which is determined based on the effective signal range that sensors can observe [8], [32]. In order to provide an unbiased estimate for θ_k , we use the probabilistic quantization scheme from [32], where \mathcal{M}_R is divided into $2^{b_i^k}$ equal intervals of length $\Delta_i^k = \frac{2M}{2^{b_i^k}}$, and the measurement $n\Delta_i^k \leq m_i^k \leq (n+1)\Delta_i^k$ is mapped to its quantization $y_i^k \doteq \mathcal{Q}(m_i^k)$ using the probabilities

$$\begin{aligned} P(y_i^k = n\Delta_i^k) &= 1 - \frac{m_i^k - n\Delta_i^k}{\Delta_i^k} \\ P(y_i^k = (n+1)\Delta_i^k) &= 1 - P(y_i^k = n\Delta_i^k). \end{aligned} \quad (3)$$

The quantization error variance for this method is given by

$$\varrho_i^k(b_i^k) = \frac{M^2}{(2^{b_i^k} - 1)^2}. \quad (4)$$

A larger value of b_i^k leads a smaller quantization error variance $\varrho_i^k(b_i^k)$ and thus provides a higher accuracy of detection, but at the cost of consuming more energy and bandwidth for transmitting more data bits to the sink. For brevity of notation, we define

$$\pi_i^k \doteq \sigma_i^2 + \varrho_i^k(b_i^k) \quad (5)$$

as effective measurement variance and omit the explicit dependence of π_i^k on b_i^k .

We assume that each sensor performs sensing at regular intervals of length T_s . Accordingly, we define the *generation rate* of node s_i for event e_k as

$$r_i^k \doteq b_i^k/T_s. \quad (6)$$

Clearly, a node can tradeoff between accuracy and energy consumption by varying its generation rate.

As it is shown in [8], [32], the quantized measurements of y_i^k , $i = 1, \dots, N$, generated by mapping (3) enable an unbiased estimation of θ_k under hypothesis H_1^k . The corresponding quasi-best linear unbiased estimator (Q-BLUE) of θ_k is specified as

$$\bar{\theta}_k = \left(\sum_{i=1}^N \frac{1}{\sigma_i^2 + \varrho_i^k(b_i^k)} \right)^{-1} \sum_{i=1}^N \frac{y_i^k}{\sigma_i^2 + \varrho_i^k(b_i^k)}. \quad (7)$$

This is essentially the same as the BLUE estimator given unquantized data, except that the quantization variance $\varrho_i^k(b_i^k)$ is added to the noise variance σ_i^2 .

We assume that the sensing interval T_s is chosen such that the value of θ_k is changing much slower than the sensing rate. Under this assumption, the filtered estimate

$$\hat{\theta}_k(\ell) = \delta \hat{\theta}_k(\ell-1) + (1-\delta) \bar{\theta}_k, \quad (8)$$

is used for determining the likelihood of hypothesis H_1^k in the current sensing interval ℓ , where $\hat{\theta}_k(\ell-1)$ is the estimate from the previous interval $\ell-1$ and $\delta < 1$ is a forgetting factor to account for dynamics of θ_k . For brevity, we omit the interval index ℓ in the following and denote the updated estimate by $\hat{\theta}_k$.

Given the described estimation procedure, deciding between H_0^k and H_1^k is performed using the generalized log-likelihood ratio test (GLRT) [17], [33]

$$L^k \underset{H_0^k}{\overset{H_1^k}{\geq}} T_0^k, \quad (9)$$

where L_k is given by

$$L^k = \log \frac{\Pr(H_1^k | y_1^k, \dots, y_N^k, \hat{\theta}_k)}{\Pr(H_0^k | y_1^k, \dots, y_N^k)}. \quad (10)$$

Here, the threshold T_0^k is determined by the DRs. More details about the detection procedure will be provided in Section III.

B. Transmission Model

Transmission of quantized measurements is performed using a TH-IR-UWB physical layer. As stated earlier, TH-IR-UWB requires a very low transmission power. In addition, it is fairly robust to interference when time hopping codes are used for the transmission of UWB pulses. Based on these properties, it is shown in [34] that power control is not required and each UWB node should transmit with the maximum permissible power. Motivated by this result, we assume that all sensors transmit with a fixed transmission power P_{tx} . Furthermore, we make use of the low spectral efficiency property of TH-IR-UWB and approximate the link capacity as a linear function of SINR [25]. That is, we express the maximum achievable rate C_{ij} for transmission from s_i to s_j as

$$C_{ij} = \frac{W}{\ln 2} \mu_{ij}, \quad (11)$$

where W is the bandwidth and μ_{ij} denotes the SINR for this link. The latter is given by

$$\mu_{ij} = \frac{P_{tx} \alpha_{ij}}{\sigma_j^2 + \chi \sum_{l \in \mathcal{N}_j \setminus \{i\}} I_l^{tx} P_{tx} \alpha_{lj}}, \quad (12)$$

where I_l^{tx} determines if node l is a potential interferer, i.e., $I_l^{tx} = 1$ if s_l is transmitting, and $I_l^{tx} = 0$ otherwise. The parameter χ is a constant depending on the autocorrelation of the UWB pulse, and α_{ij} denotes the path gain between nodes s_i and s_j . For the latter, we adopt the double-slope UWB channel model developed during IEEE 802.15.4a standardization [35], [36], according to which

$$\alpha_{ij}(d_{ij}) = \begin{cases} g - 10\gamma_1 \log_{10}(d_{ij}) & d_{ij} \leq d_0, \\ c_0 - 10\gamma_2 \log_{10}(d_{ij}/d_0) & d_{ij} > d_0, \end{cases} \quad (\text{in dB}), \quad (13)$$

where g is the gain for the unit distance, c_0 is the gain for the reference distance d_0 , and γ_1, γ_2 are the path-loss exponents. The SINR term in (12) along with the path gain model (13) are used in this paper for computing the link capacities. We note, however, that other channel models could be used in our optimization framework.

The indicator terms I_l^{tx} in (12) are determined by the scheduling of transmissions in the network. The joint scheduling and routing problem in UWB has been investigated in [25], [28], [34]. In these studies, it is shown that finding the optimal scheduling policy to achieve a given objective, such as minimum power consumption or

maximum throughput, is in general NP-hard to solve, and different techniques for finding an approximate solution are suggested. The simpler interference-free scheduling, in which separate subbands or time slots are assigned to links that would otherwise cause interference to each other, is often assumed when lifetime maximization is done at the routing layer [7], [8], [14]. In this case, the second term in the denominator of SINR (12) would vanish and a larger capacity would be obtained, at the cost of synchronizing the nodes and providing orthogonal resources (time, frequency, etc.). Since the UWB PHY provides robustness to interference (see (12)), carefully designed interference-free scheduling is not required. However, since including the exact effect of the scheduling policy significantly increases the complexity of optimizing the routing layer [25], [28], [34], in this work we resort to consider two extreme cases. The first is the capacity lower bound C_{ij}^L assuming maximum interference according to $I_l^{tx} = 1, \forall l \in \mathcal{N}_j$, and the second is the capacity upper bound C_{ij}^U assuming $I_l^{tx} = 0, \forall l \in \mathcal{N}_j$ in (12). This simplification allows us (i) to provide a simplified model for lifetime optimization in UWB-based WSNs, (ii) to fairly compare the proposed framework to the existing literature which implicitly uses the scheduling with no interference (i.e., C_{ij}^U) [7], [8], and (iii) to adapt the distributed routing framework [14] to the problem at hand.

Finally, we consider dynamic channel coding [20], [22], [23]. This technique adaptively adjusts the channel code rate according to the level of interference. This allows us to express the energy consumed for the transmission of one bit from s_i to s_j as

$$E_{tx} = \frac{P_{tx}}{C_{ij}}. \quad (14)$$

C. Routing

Let f_{ij}^k be the data flow from s_i to s_j for event e_k . Then, the flow conservation constraints are given by

$$r_i^k + \sum_{j \in \mathcal{N}_i} f_{ji}^k - \sum_{j \in \mathcal{N}_i} f_{ij}^k = 0, \quad \forall i, k. \quad (15)$$

Since all the flow is absorbed by the sink, the flow conservation is valid for the sink node by defining

$$r_o^k = - \sum_{i=1}^N r_i^k, \quad (16)$$

and noting that $f_{oi}^k = 0, \forall i, k$.

It is worth mentioning that the fraction of time taken for the transmission of each flow is f_{ij}^k / C_{ij} . Thus, a feasible scheduling can be obtained for the high interference case if

$$\sum_i \sum_j \sum_k \frac{f_{ij}^k}{C_{ij}} \leq T_s. \quad (17)$$

This is also a sufficient condition for the existence of a feasible schedule in the interference-free with the capacity upper bound C_{ij}^U .

D. The Optimization Procedure

Based on the sensing, transmission, scheduling, and routing models explained above, a centralized and a distributed optimization of sensor rates r_i^k and flows f_{ij}^k are devised in the next two sections. Figure 3 shows a flowchart of the proposed centralized and distributed algorithms. As can be seen, in both methods the sink performs the GLRT to decide for H_0^k or H_1^k , and updates the estimate for θ_k if the event e_k is deemed present. In the centralized scheme, the sink also optimizes all routing variables and generation rates. Since the optimization of these parameters depends on the estimate $\hat{\theta}_k$ of θ_k , as will be explained in Section III, the sink needs to repeat the

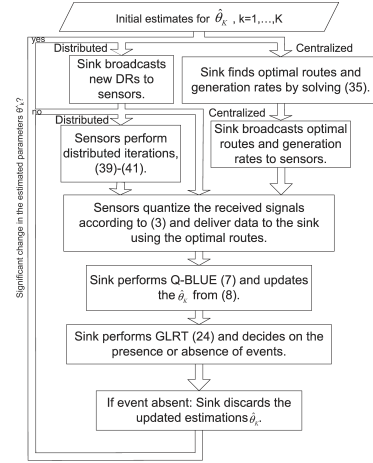


Fig. 3. Flowchart of the proposed centralized and distributed lifetime maximization algorithms.

optimization whenever the current estimate is notably different from the estimate used previously for optimization. Since we assume that θ_k is changing slowly compared to T_s , the optimization by the sink is performed infrequently. Furthermore, since no *a priori* model for the dynamics of θ_k is assumed to be known, the optimization by the sink needs to be performed in a myopic fashion. The routing and generation rate optimizations in the distributed scheme are performed locally in each sensor, and the optimized local variables only need to be exchanged among the neighboring nodes. However, the sink needs to broadcast the estimates $\hat{\theta}_k$ in the network when notable changes of these estimates occur.

In the next section, we present the centralized UWB maximum lifetime for joint event-detection (UMLJE) algorithm. Its distributed version, referred to as D-UMLJE, is developed in Section IV.

III. UWB MAXIMUM LIFETIME FOR JOINT EVENT DETECTION (UMLJE)

In UMLJE, the sink determines the generation rates and routing flows such that network lifetime is maximized and the DRs are satisfied. In this section, we first make the implementation of the GRLT from (10) explicit. Then we formalize the DRs as functions of generation rates and map them to equivalent convex constraints. Using these constraints, we devise a convex program for the lifetime maximization problem. For the derivation of the GLRT and DRs we closely follow [7], but we note that [7] did not consider quantization of measurements at sensor nodes.

A. Closed-form Expression for the GLRT

In order to obtain a closed-form expression for the GLRT, we approximate y_i^k as a Gaussian distributed random variable with variance π_i^k and mean 0, if H_0^k , and mean $\hat{\theta}_k$, if H_1^k , where $\hat{\theta}_k$ is the current estimation for θ_k given by (8). Then, according to the sensing model from Section II-A, the generalized likelihood ratio L^k in (10) can be approximated as

$$L^k = \sum_{i=1}^N \frac{1}{2\pi_i^k} \left(2\hat{\theta}_k y_i^k - \hat{\theta}_k^2 \right). \quad (18)$$

Therefore, the hypothesis test (9) follows as

$$\sum_{i=1}^N \frac{\hat{\theta}_k y_i^k}{\pi_i^k} \underset{H_0^k}{\overset{H_1^k}{\geq}} T_0^k + \sum_{i=1}^N \frac{\hat{\theta}_k^2}{2\pi_i^k}. \quad (19)$$

It is convenient to make the following definitions:

$$\psi_i^k \doteq \frac{\hat{\theta}_k^2}{\pi_i^k} \quad (20)$$

$$\psi^k \doteq \sum_i \psi_i^k \quad (21)$$

$$h^k \doteq \sum_{i=1}^N \frac{\hat{\theta}_k y_i^k}{\pi_i^k} \quad (22)$$

$$T_1^k \doteq \left(T_0^k + \frac{1}{2} \sum_{i=1}^N \psi_i^k \right). \quad (23)$$

Then, the GLRT (19) can be expressed in the compact form

$$h^k \underset{H_0^k}{\overset{H_1^k}{\geq}} T_1^k. \quad (24)$$

B. Detection Requirements

The DRs for event-detection applications are given in terms of the probability of detection

$$p_d^k \doteq \Pr(L^k > T_0^k | H_1^k), \quad (25)$$

if event e_k is present (hypothesis H_1^k) and the probability of false alarm

$$p_f^k \doteq \Pr(L^k > T_0^k | H_0^k), \quad (26)$$

if e_k is absent (hypothesis H_0^k). Specifically, we focus on the Neyman-Pearson detection model [7], [16], where $p_f^k = \nu^k$ and $p_d^k \geq \eta^k$ should be satisfied for some thresholds ν^k and η^k . That is, the threshold T_0^k in (9) is obtained by solving $p_f^k = \nu^k$ [17]. In the following, we elaborate on this relationship, which also relates the DR parameters ν^k and η^k to the sensor generation rates r_i^k .

The random variable h^k defined in (22) has the variance ψ^k , and zero mean, if H_0^k , and mean $\frac{\hat{\theta}_k \theta_k}{\pi_i^k}$, if H_1^k . Since $\hat{\theta}_k$ approximates θ_k , we assume that $E(h^k | H_1^k) \simeq \psi^k$. Denoting by φ the cumulative distribution function (cdf) of the ‘‘standard’’ h^k , i.e., when its mean and variance are adjusted to 0 and 1, respectively, and using (24) in (26), the false alarm probability can be expressed as

$$p_f^k = 1 - \varphi \left(\frac{T_1^k - 0}{\sqrt{\psi^k}} \right). \quad (27)$$

Since φ is not a one-to-one function due to the quantization step, we first need to define its inverse in an unambiguous manner. Let for values of $\{x_0 < x_1 < \dots < x_{n+1}\}$, $\{p_0 = 0 < p_1 < \dots < p_n = 1\}$ be the set of values that $\varphi(x)$ can take, i.e., $x_i \leq x < x_{i+1} \Leftrightarrow \varphi(x) = p_i$. For $p_i \leq p < p_{i+1}$ we define two inverse functions, $\varphi_{\downarrow}^{-1}(p) \doteq x_i$ and $\varphi_{\uparrow}^{-1}(p) \doteq x_{i+1}$. Then, setting $p_f^k = \nu^k$ leads to the detection threshold

$$T_1^k = \sqrt{\psi^k} \varphi_{\uparrow}^{-1} \left(1 - \nu^k \right), \quad (28)$$

where the use of φ_{\uparrow} causes the achieved false alarm probability not to be larger than the desired ν^k . Similarly, from the demanded detection accuracy $p_d^k \geq \eta^k$ it follows that

$$1 - \varphi \left(\frac{T_1^k - \psi^k}{\sqrt{\psi^k}} \right) \geq \eta^k. \quad (29)$$

This implies that in order to meet the DR constraints, the following condition should be satisfied:

$$\psi^k \geq \xi_k^2 \doteq \left(\varphi_{\uparrow}^{-1}(1 - \nu^k) - \varphi_{\downarrow}^{-1}(1 - \eta^k) \right)^2, \quad (30)$$

where the use of φ_{\downarrow} results in an achieved detection probability which is never smaller than η^k . The expression in (30), through (20), (21), (5), and (6), links the generation rates r_i^k to the DRs.

Finally, we show that for any given ξ_k^2 , the expression in (30) can also be written as an equivalent constraint.

Proposition 1: Define

$$\rho^k \doteq \left(\sum_{i=1}^N \frac{1}{\pi_i^k} \right)^{-1}, \quad \zeta^k \doteq \frac{\hat{\theta}_k^2}{\xi_k^2}. \quad (31)$$

Then, the DR constraint in (30) can be equivalently written as

$$\rho^k \leq \zeta^k. \quad (32)$$

Proof: Introducing the definitions (20), (21), and (31) into the inequality (30), we obtain

$$\rho^k = \left(\sum_{i=1}^N \frac{1}{\pi_i^k} \right)^{-1} = \left(\sum_{i=1}^N \frac{\psi_i^k}{\hat{\theta}_k^2} \right)^{-1} = \frac{\hat{\theta}_k^2}{\psi^k} \leq \frac{\hat{\theta}_k^2}{\xi_k^2} = \zeta^k. \quad \blacksquare$$

Proposition 1 states that the constraints (30) and (32) can be equivalently used to account for the DRs. Note that any value of ζ^k can be mapped to specific DRs at a given event signal-to-noise ratio (SNR), i.e., θ_k^2/σ_i^2 . As the DRs become stricter, ζ^k becomes smaller and hence sensors need to generate more bits per measurement in order to reduce ρ^k and satisfy (32).

While constraints (30) and (32) can be used interchangeably, it turns out that unlike (30), the expression (32) leads to a convex formulation of the DRs in the generation rates [37]. This can be verified by computing the Hessian matrix of ρ^k with respect to variables r_i^k and noting that it is positive definite for $r_i^k \geq \kappa_0$, where $\kappa_0 > 0$ is a small threshold. It is also worth mentioning that ρ^k represents an upper bound on the mean square error (MSE) of the Q-BLUE estimation in (7) [8], [32].

C. Operational Lifetime

We are interested in finding the maximum time during which the network is able to detect given events with the required detection probabilities, which we define as the operational lifetime of the network.

Let t_i denote the operational lifetime of node s_i during which it is able to perform sensing and routing for the events before its energy E_i is depleted. We can express t_i as

$$t_i = \frac{E_i}{\sum_k \left(I_{ik}^s \frac{E_s}{T_s} + \sum_j f_{ji}^k E_{rx} + \sum_j f_{ij}^k (E_p + E_{tx}) \right)}, \quad (33)$$

where E_s , E_{rx} , and E_p is the energy consumed for sensing, receiving a bit, and processing a bit, respectively. In (33), $I_{ik}^s = 1$ only if s_i performs sensing for the event e_k , and the terms in the denominator correspond to the energy consumed for sensing, receiving, and transmitting data, respectively, in each sensing interval. The operational lifetime of the network T is then defined as the minimum lifetime among the nodes:

$$T \doteq \min_i t_i. \quad (34)$$

Defining the inverse of the lifetime, $q \doteq \frac{1}{T}$, lifetime maximization can be written as the following optimization problem:

$$\min_{q, r_i^k, f_{ij}^k} q \quad \text{subject to} \quad (35a)$$

$$r_i^k + \sum_j f_{ji}^k - \sum_j f_{ij}^k = 0, \forall i, k \quad (35b)$$

$$\sum_k \left(I_{ik}^s \frac{E_s}{T_s} + \sum_j f_{ji}^k E_{rx} + \sum_j f_{ij}^k (E_p + E_{tx}) \right) \leq q E_i, \forall i \quad (35c)$$

$$\frac{\left(\sum_{i=1}^N \frac{1}{\sigma_i^2 + \frac{M^2}{(2^{r_i^k} - 1)^2}} \right)^{-1}}{\hat{\theta}_k^2} \leq \frac{\varphi_{\uparrow}^{-1}(1 - \nu^k) - \varphi_{\downarrow}^{-1}(1 - \eta^k)}{2}, \forall k \quad (35d)$$

$$0 \leq r_i^k \leq \frac{b_{\max}}{T_s}, \forall i, k \quad (35e)$$

$$0 \leq q, \quad (35f)$$

$$0 \leq f_{ij}^k, \forall i, j, k. \quad (35g)$$

In (35), the constraint (35b) ensures flow conservation, and the constraint (35c) gives the local energy consumption in the nodes based on (33). Note that in each node, the total energy consumption for detecting, sensing, and reporting of all events is jointly considered. Since this constraint also considers the total flow for multiple events, the optimal solution will efficiently avoid the bottleneck situations which would occur if single event detection methods like [7], [8] were applied. Consequently, the optimal solution will balance the energy consumption for sensing and communicating among the UWB-enabled sensors to achieve the highest operational lifetime. In addition, the DR constraint (35d) ensures that the DRs in (30) are satisfied as well. Numerical evidence and quantitative results of these properties are provided in Section V, specifically, in Figures 4, 6, and 8. Finally, the last three constraints give the range of variables. While (35d) is written in terms of optimization variables, for brevity, we will use the compact form (32) in the following.

Furthermore, note that in the optimization (35), we consider continuous variables r_i^k . From the solution, we obtain b_i^k by rounding to the nearest integer. Consequently, all the constraints except (35d) are linear and simple to handle for optimization routines. These constraints are also typically considered in existing lifetime maximization frameworks such as [13], [14]. Moreover, the DR constraint (35d), which is unique to our problem, is also convex in the variables r_i^k . Hence, (35) is a convex optimization problem and can efficiently be solved by standard methods. Since the DR constraint (35d) depends on the value of $\hat{\theta}_k$, a new optimization should be performed by the sink if these parameters have notably changed over time.

IV. EXTENSION TO DISTRIBUTED OPTIMIZATION

In this section, we devise a distributed version of UMLJE, which we refer to as D-UMLJE. To this end, we apply a dual decomposition method similar to the one from [14] and [38], which decomposes problem (35) into local subproblems by means of Lagrangian relaxation. These problems are solved by exchanging Lagrange multipliers between nodes and updating the variables based on the subgradient method. This process is continued until the variables converge to their global optimal point, i.e., when the subgradient method is unable to improve the current values of the local variables.

A. Distributed UMLJE (D-UMLJE)

To explain this in more detail, we start with the regularized objective

$$J_{\text{reg}} = q^2 + \epsilon \sum_{i,j,k} (f_{ij}^k)^2, \quad (36)$$

where ϵ is the regularization weight. Note that the all terms in the objective function are differentiable. The Lagrangian relaxation can then be used to obtain the following regularized decomposition of the original problem in (35):

$$\begin{aligned} \min_{q, r_i^k, f_{ij}^k} \quad & q^2 + \epsilon \sum_{i,j,k} (f_{ij}^k)^2 + \sum_{k=1}^K \omega^k (\rho^k - \zeta^k) \\ & + \sum_{i,k} \lambda_i^k \left(-r_i^k - \sum_j f_{ji}^k + \sum_j f_{ij}^k \right) \\ & + \sum_i \tau_i \left(\sum_k \left(I_{ik}^s \frac{E_s}{T_s} + \sum_j f_{ji}^k E_{rx} + \sum_j f_{ij}^k (E_p + E_{tx}) \right) - q E_i \right) \end{aligned} \quad (37a)$$

$$\text{subject to} \quad 0 \leq r_i^k \leq \frac{b_{\max}}{T_s}, \quad (37b)$$

$$0 \leq q, \quad (37c)$$

$$0 \leq f_{ij}^k, \quad (37d)$$

where Lagrange multipliers λ_i^k , τ_i , and ω^k correspond to constraints (35b), (35c), and (35d) of the original problem, respectively. Problem (37) is analogous to the distributed problem in [14, Sec. IV.C], but here the variables ω^k enable us to account for the DR constraints. Note that the objective (37a) is locally separable over flow variables f_{ij}^k . In other words, nodes can optimize the flow variables by exchanging the Lagrange multipliers λ_i^k and τ_i only between their neighbors. However, this fact does not hold for the variables q and ρ^k , and the Lagrange multipliers ω^k . Hence, problem (37) is a *partially separable distributed optimization* [14]. In order to map (37) to its fully distributed equivalent, we need to define local variables q_i and ρ_i^k and solve the following optimization:

$$\begin{aligned} \min_{q_i, r_i^k, f_{ij}^k} \quad & \sum_i q_i^2 + \epsilon \sum_{i,j,k} (f_{ij}^k)^2 + \sum_{i,k} \omega_i^k (\rho_i^k - \zeta^k) \\ & + \sum_{i,k} \lambda_i^k \left(-r_i^k - \sum_j f_{ji}^k + \sum_j f_{ij}^k \right) \\ & + \sum_i \tau_i \left(\sum_k \left(I_{ik}^s \frac{E_s}{T_s} + \sum_j f_{ji}^k E_{rx} + \sum_j f_{ij}^k (E_p + E_{tx}) \right) - q_i E_i \right) \\ & + \sum_{i,j} \Lambda_{ij} (q_i - q_j) + \sum_{i,j,k} \Upsilon_{ij}^k (\rho_i^k - \rho_j^k) \end{aligned} \quad (38a)$$

$$\text{subject to} \quad 0 \leq r_i^k \leq \frac{b_{\max}}{T_s}, \quad \forall i, k \quad (38b)$$

$$0 \leq q_i, \quad \forall i, \quad (38c)$$

$$0 \leq f_{ij}^k, \quad \forall i, j, k, \quad (38d)$$

where the objective is summed over the newly-defined local variables, and the last two terms in the objective are inserted in order to force the local variables q_i and ρ_i^k to be equal to their global value. After this modification, every single term in the objective (38a) is separable over all variables q_i , r_i^k , f_{ij}^k and Lagrange multipliers λ_i^k , τ_i , ω_i^k , Λ_{ij} , Υ_{ij}^k . However, note that the value of ζ^k , which is independent of local variables, needs to be broadcasted to all nodes whenever a significant change in $\hat{\theta}^k$ is observed, and therefore D-UMLJE is not

fully distributed in the strict sense. But since D-UMLJE is distributed as far as the solution of the optimization problem is concerned, we refer to D-UMLJE as a distributed solution similar to [14].

The distributed problem (38) is solved using the subgradient method. At each iteration, the sensor s_i solves the localized part of (38) with only the terms involving its own variables using the current values of Lagrangian multipliers obtained from the previous iteration. Mathematically, at iteration ℓ

$$\begin{aligned} q_i(\ell) &= \underset{0 \leq q_i \leq Q}{\operatorname{argmin}} \left(q_i^2 - q_i \left(E_i \tau_i + \sum_{j \in \mathcal{N}_i} (\Lambda_{ij} - \Lambda_{ji}) \right) \right), \quad \forall i, \\ f_{ij}^k(\ell) &= \underset{0 \leq f_{ij}^k}{\operatorname{argmin}} \epsilon \sum_{k=1}^K (f_{ij}^k)^2 + \sum_{k=1}^K f_{ij}^k \left((\lambda_i^k - \lambda_j^k) \right. \\ &\quad \left. + \tau_i (E_p + E_{tx}) + \tau_j E_{rx} \right), \quad \forall i, j \in \mathcal{N}_i, \\ r_i^k(\ell) &= \underset{0 \leq r_i^k \leq \frac{b_{\max}}{T_s}}{\operatorname{argmin}} \left(\rho_i^k \left(\omega_i^k + \sum_{j \in \mathcal{N}_i} (\Upsilon_{ij}^k - \Upsilon_{ji}^k) \right) \right. \\ &\quad \left. - r_i^k \lambda_i^k \right), \quad \forall i, k, \end{aligned} \quad (39)$$

where Q is a loose upper bound for q_i and all the terms in right hand side are from iteration $\ell - 1$. Also, according to the definition of ρ_i^k in (31), the values of $\rho_i^k(\ell)$ are updated as

$$\rho_i^k(\ell) = \left(\frac{1}{\rho_i^k(\ell-1)} - \frac{1}{\pi_i^k(\ell-1)} + \frac{1}{\pi_i^k(\ell)} \right)^{-1}, \quad (40)$$

where $\pi_i^k(\ell-1)$ and $\pi_i^k(\ell)$ are the variances corresponding to $r_i^k(\ell-1)$ and $r_i^k(\ell)$ defined in (5). We observe that optimization over q_i , f_{ij}^k , and r_i^k takes place separately. In addition, the optimization for q_i and f_{ij}^k are in the form of a quadratic functions, for which closed-form solutions exist.

Finally, the update rules for Lagrange multipliers based on the subgradient method are given by

$$\begin{aligned} \omega_i^k(\ell) &= \left(\omega_i^k(\ell-1) + u(\ell-1) (\zeta^k - \rho_i^k) \right)_+, \\ \lambda_i^k(\ell) &= \lambda_i^k(\ell-1) + u(\ell-1) \left(r_i^k + \sum_j f_{ji}^k - \sum_j f_{ij}^k \right), \\ \tau_i(\ell) &= \left(\tau_i(\ell-1) + u(\ell-1) \left(q_i E_i - \sum_k \left(I_{ik}^s \frac{E_s}{T_s} \right. \right. \right. \\ &\quad \left. \left. \left. - \sum_j f_{ji}^k E_{rx} - \sum_j f_{ij}^k (E_p + E_{tx}) \right) \right) \right)_+, \\ \Lambda_{ij}(\ell) &= \Lambda_{ij}(\ell-1) + u(\ell-1) (q_i - q_j), \\ \Upsilon_{ij}^k(\ell) &= \Upsilon_{ij}^k(\ell-1) + u(\ell-1) (\rho_i^k - \rho_j^k), \end{aligned} \quad (41)$$

where $u(\ell)$ is a decreasing function of ℓ , and $(\cdot)_+$ maps the negative values to 0 [14], [39]. Note that the Lagrange multipliers are updated using the results of optimizations in (39) at the same iteration. The convergence of the above-mentioned subgradient method to the optimal solution of the problem (38) can be shown using the same arguments as [14]. Furthermore, strong duality holds between the UMLJE (35) and the un-regularized D-UMLJE (i.e., (38) with $\epsilon = 0$). Hence, choosing a small regularization weight ϵ allows us to closely approximate the optimal solution of the UMLJE. (See [14, Sections IV and V] and references therein for further details.)

B. Discussion

1) *Overhead Comparison:* As stated earlier, both UMLJE and D-UMLJE schemes incur signalling overhead for exchanging the information with the sink or their neighboring nodes. The major

overhead in UMLJE comes from the initial collection of SINR values in the sink. Also, the optimized data need to be sent by the sink to each node. Hence, we have $O(\Gamma)$ two-way transmissions between nodes and sink per node, where Γ is the average network depth, i.e., the average number of hops that a node needs for connecting to the sink. On the other hand, D-UMLJE only requires $O(E)$ communications per node per iteration for exchanging optimization variables, where E is the average number of neighbors of a node in the network. For a fixed density, Γ grows with network size N , but E is independent of N , which renders D-UMLJE scalable with regards to message exchange for optimization, and thus better suited than UMLJE for larger networks. However, denser topologies would lead to an increased packet exchange between neighbors for local optimization in D-UMLJE. Finally, as mentioned above, K variables ζ^k in D-UMLJE and the optimization results in UMLJE need to be broadcasted by the sink.

With regards to computational complexity, the problem (35) is more computationally-involved than each round of the distributed optimizations (39)-(41). Specifically, solving the convex optimization (35) in a centralized manner has a computational complexity of $O(N^3)$, while the complexity of each distributed update iteration is $O(1)$ at every node. Our simulations indicate that the number of iterations needed for D-UMLJE to converge is typically $O(N)$. Hence, unless the sink has considerably more computational resources than the other sensor nodes, D-UMLJE is preferable in terms of complexity.

2) *Dynamics of θ^k :* If no prior knowledge is available, $\hat{\theta}^k$ can be initialized arbitrarily. (For the numerical results reported in the next section, we initialize it as 0). Through the choice of the forgetting factor δ , we can trade-off speed of convergence towards the true value θ^k and steady-state accuracy of the estimate. However, an uninformed initialization of $\hat{\theta}^k$ is only needed at a first acquisition, then this parameter can be tracked. This also means that δ could be chosen smaller during acquisition, and then larger in the tracking phase. Since updates of the estimate of θ^k also lead to broadcasts from the sink for updating ζ^k in D-UMLJE and of optimization results in UMLJE, there is a tradeoff between tracking accuracy of θ^k and energy consumption for communicating parameter updates.

V. PERFORMANCE EVALUATION

In this section, we examine the performance of the proposed UMLJE and D-UMLJE approaches and compare them with previously proposed maximum lifetime and event detection methods, namely, MERG [7, Alg. 2], MLB [8], and URFP [28, Figure 2]. Recall that MERG finds the minimum energy routes that satisfy the DRs. The best route is obtained by maximizing a lower bound for lifetime. URFP connects the source nodes to the sink through the links with the highest data rates. Finally, MLB tries to maximize an upper bound for lifetime by decoupling the quantization and routing problems. Since the decoupled routing problem in MLB is identical to the routing problem in URFP, MLB and URFP use the same set of routes. We also note that for URFP and MERG, there is no notion of quantization bits b_i^k , and we equally divide the required bits between the nodes in the sensing range of an event. In the simulations, we always apply the interference-free scheduling to MERG, MLB and URFP.

Table I summarizes the parameters used for the simulations. For the UWB channel model, the non-line-of-sight (NLOS) indoor office environment is assumed [36]. The energy consumption parameters are chosen according to a typical UWB device [20], [40]. In the simulations, the number of nodes varies from $N = 10$ to $N = 50$ for detecting $K = 2$ events. Unless otherwise specified, all sensors are assumed to experience the same noise variance, and the default

TABLE I
SIMULATION PARAMETERS

Parameter	Value	Parameter	Value
γ_1	2.0	γ_2	3.07
d_0	4 m	g	-60 dB
G	1	D	12 m
P_{tx}	-14.3 dBm	T_s	1 Sec.
E_{rx}	2.5 nJ/bit	E_p	10 pJ/bit
E_i	10 J	E_s	10 nJ
W	1.0 GHz	σ_i^2	-84 dBm
K	2 - 5	N	10 - 50
δ	0.9	χ	0.08
Simulation runs	100	b_{\max}	12 bits
ϵ	$\max\{0.1, \exp(-\frac{\ell}{10})\}$	$u(\ell)$	$\max\{0.01, \frac{0.5}{\sqrt{\ell}}\}$
$\frac{M^2}{\sigma^2}$	50.0 dB	$\frac{\theta^2}{\sigma^2}$	37.0 dB

detection requirements are set to $\eta^k = 0.90$ and $\nu^k = 0.10$. We assume that the parameters θ_k remain constant with an SNR of $\frac{\theta_k^2}{\sigma_k^2} = 37.0$ dB $\forall i, k$, and are perfectly estimated, i.e., $\hat{\theta}_k = \theta_k$, $k = 1, \dots, K$.

A. A Sample Scenario

We first consider an example with $N = 25$ nodes and $K = 2$ events shown in Figure 4. In this figure, sensor nodes are represented by circles, and the events, which are located at the right corners, are identified by the squares. The sink is located at the lower left corner. For this example, we apply the interference-free scheduling with detection requirements of ($\eta^k = 0.97$, $\nu^k = 0.03$). The set of routes found by URFP, MERG, and the proposed UMLJE are shown in Figures 4(a), 4(b), and 4(c), respectively. As stated previously, URFP routes also represent the MLB routes. The numbers in the brackets in Figure 4 show the number of quantization bits b_i^k at each node and the numbers in the parentheses show the amount of flow in the link for each event. Each line's thickness is proportional to the amount of flow on the corresponding link. In Figure 4(c), arrows are used for indicating the direction of flows in the network.

As can be seen from Figure 4(c), the total flow for jointly detecting e_1 and e_2 is completely distributed between the nodes in the network core, i.e., the nodes in the transmission range of the sink. Specifically, in UMLJE there are 4 nodes that transmit to the sink, while in Figures 4(a) and 4(b) only 1 node transmits to the sink. The balance of flows in the network core causes this nodes to run out of energy almost at the same time, and thus avoids the bottleneck problem. Note that, following the arrows in Figure 4(c), it can be observed that UMLJE directs a fare proportion of flow generated from e_1 downwards, in order to balance the flow between the three core nodes that carry traffic from this part of the network. Note that in UMLJE, the number of quantization bits for estimating an event may vary among sensors. This is because UMLJE jointly optimizes the quantization and routing problems, hence quantization bits are adjusted according to the optimal routes. On the other hand, MLB decouples the quantization problem and thus the quantization bit assignments are independent of the routes. Since the network is homogeneous, i.e., noise variances are the same, MLB assigns the same number of quantization bits to different sensors.

B. Performance Comparison

Figure 5 compares the maximum lifetime obtained from UMLJE and D-UMLJE with $K = 2$ events when the number of nodes

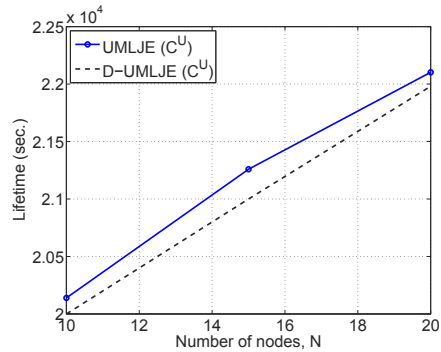


Fig. 5. Network lifetime of UMLJE and D-UMLJE as a function of number of nodes for $K = 2$ events.

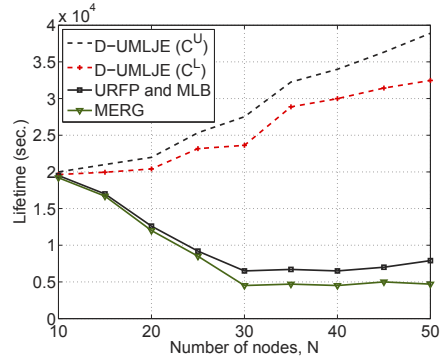


Fig. 6. Network lifetime of MERG, URFP and D-UMLJE as a function of network size N for $K = 2$ events.

vary from 10 to 20 under the interference-free scheduling C^U . In D-UMLJE, a node stops its local updates if for all variables the difference between the updated and previous value is less than 0.1% in ten consecutive iterations. This stopping criterion could be relaxed for an earlier stop, and to tradeoff complexity and energy consumption for optimization with performance and lifetime for event detection. As can be seen, the optimal value of D-UMLJE is very close to that for UMLJE. This fact is expected due to the strong duality between UMLJE and un-regularized D-UMLJE [14]. The small gap is due to the regularization weight. Hence, we provide a powerful lifetime maximization solution that can be implemented in a distributed manner.

For network sizes of 10 to 50 nodes, we compare the performance of D-UMLJE with URFP (also MLB) and MERG in Figure 6. In this figure, the lifetime of D-UMLJE with both lower and upper bounds of link capacities (C^L, C^U) are shown. We observe from Figure 6 that the lifetime obtained using D-UMLJE is significantly improved by increasing the number of nodes and thus node density, since in a network with larger number of nodes, the optimization is able to find more paths towards the sink and balance energy consumption among them. On the other hand, MERG fails to grab this opportunity, since after satisfying the DRs, MERG always chooses a minimum energy route regardless of its load, which is clearly not a lifetime-optimal approach in the presence of multiple events. Although the lifetime in URFP (also MLB) is slightly improved by increasing N from 40 to 50, the overall lifetime is significantly lower than that for D-UMLJE due to the fact that URFP sacrifices the lifetime by finding the routes with higher capacities. This also shows the disadvantage of MLB, which tries to maximize a loose upper bound on lifetime based on the MSE requirements.

It can also be seen from Figure 6 that the lifetime of the proposed

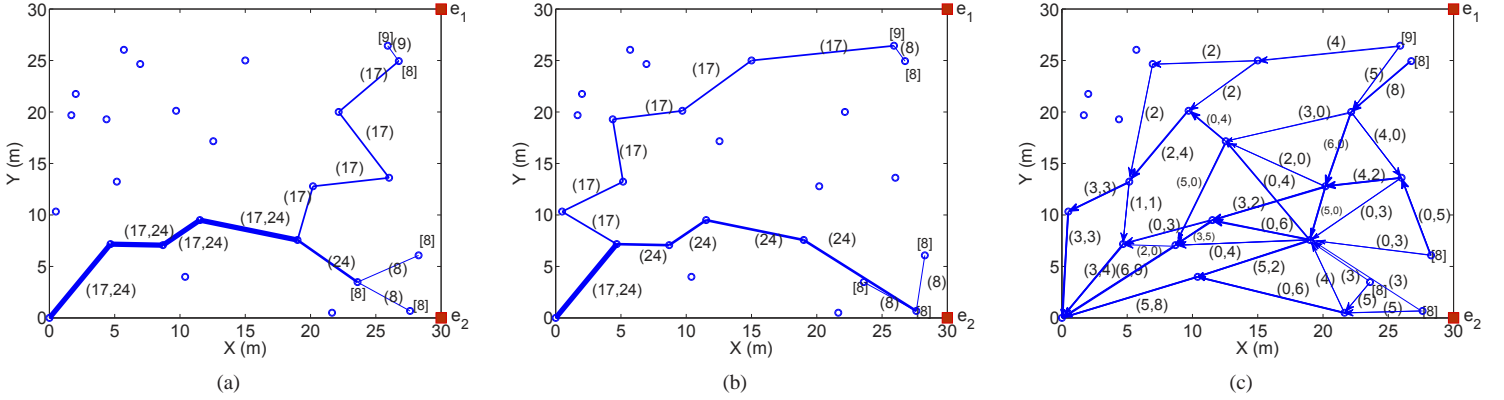


Fig. 4. Comparison between routes (a) URFP [28], (b) MERG [7], and (c) UMLJE. $N = 25$ sensor nodes (circles) detecting $K = 2$ events e_1, e_2 (squares) with DRs $\nu^k = 0.03$, $\eta^k = 0.97$. The MLB approach [8] in the homogeneous networks chooses the same routes as URFP. The sink is located at $(0,0)$, and the squares at $(30,0)$ and $(30,30)$ represent the location of events. The numbers in brackets show the optimal number of quantization bits b_i^k at each node and the numbers in the parentheses show the amount of flow in the link for each event. Each line's thickness is proportional to the amount of flow on the corresponding link. In (c), arrows are used for indicating the flow directions in the network.

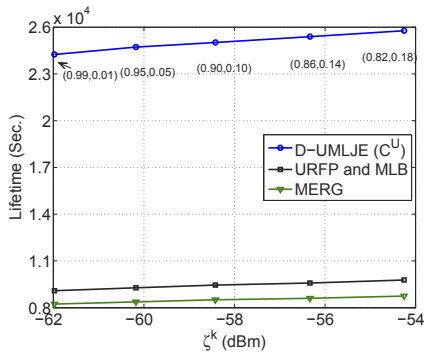


Fig. 7. Network lifetime as a function of DRs for $N = 25$ nodes and $K = 2$ events. A smaller value of ζ^k corresponds to a stricter DR, which is shown as (η^k, ν^k) for each point.

method with interference-free scheduling (C^U) is larger than that for maximum interference scenario (C^L), since in the latter the consumed transmission energy per bit is higher.

Figure 7 compares the lifetime of D-UMLJE, URFP (also MLB), and MERG for different DRs ζ^k in a network with $N = 25$ nodes and $K = 2$ events under interference-free scheduling. Note that, as explained in Section III-B, any value of ζ^k can be mapped to a specific DR at a given event SNR based on (31). These corresponding values for each ζ^k are also shown in this figure. Note that a larger ζ^k corresponds to a looser DR and hence a smaller generation rate. Therefore, lifetime increases as ζ^k increases. As can be further seen from Figure 7, for a given DR, the lifetimes of URFP, MLB, and MERG are significantly lower than that for D-UMLJE. This shows that D-UMLJE is able to find the best routing and quantization strategy for the given DR.

Figure 8 shows the detection rate achieved in a network. The detection rate should ideally match to the desired η^k assigned in the optimization, but because of the quantization of observation variables, it deviates from its ideal value. As can be seen in Figure 8, the achieved detection rate is never smaller than the assigned value of η^k and is very close to η^k for higher values, because more bits are used for reporting an event, and thus the Gaussian approximation is tighter.

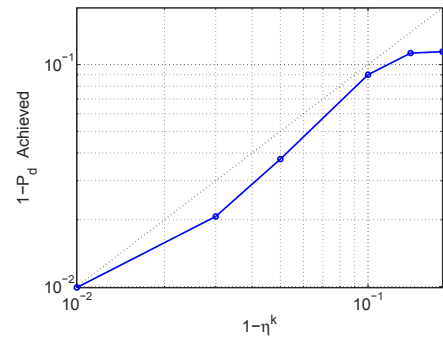


Fig. 8. Achieved detection rate as a function of the desired detection probability η^k . Dotted line shows the 45° line for reference.

C. Convergence of D-UMLJE

In this section, we present some simulation results to illustrate the convergence properties of D-UMLJE. Considering network of sizes of $N = 10, 25$, and 50 , and $K = 2$ events, we plot the variables q_i and ρ_i^k , normalized to their final values, as a function of the iteration number in Figure 9. Figure 9(a) shows the evolution of q_i for two selected sensors for each network size, and Figure 9(b) provides plots of ρ_i^k for one selected sensor for each network size. As can be seen, ρ_i^k generally converges faster than q_i . In particular, after about 100 iterations, the values for ρ_i^k are practically converged to their final value, regardless of the network size. This is because the variables ρ_i^k are only updated by the nodes in the sensing range of e_k , and thus there is no scalability issue with regards to network size N . Compared to this, the convergence of q_i requires a larger number of iterations and the convergence time increases with network size. Balancing the network traffic by adjusting the local variables q_i through local message passing eventually involves an information exchange throughout the entire network.

Figure 9(c) shows the convergence of the dual value (38a) normalized to its optimal for three scenarios of network sizes of $N = 10, 25$, and 50 . As can be seen, the convergence is fairly fast, i.e. nodes can find a solution close to the optimal one after few iterations. As expected, more number of iterations is needed for convergence in larger networks.

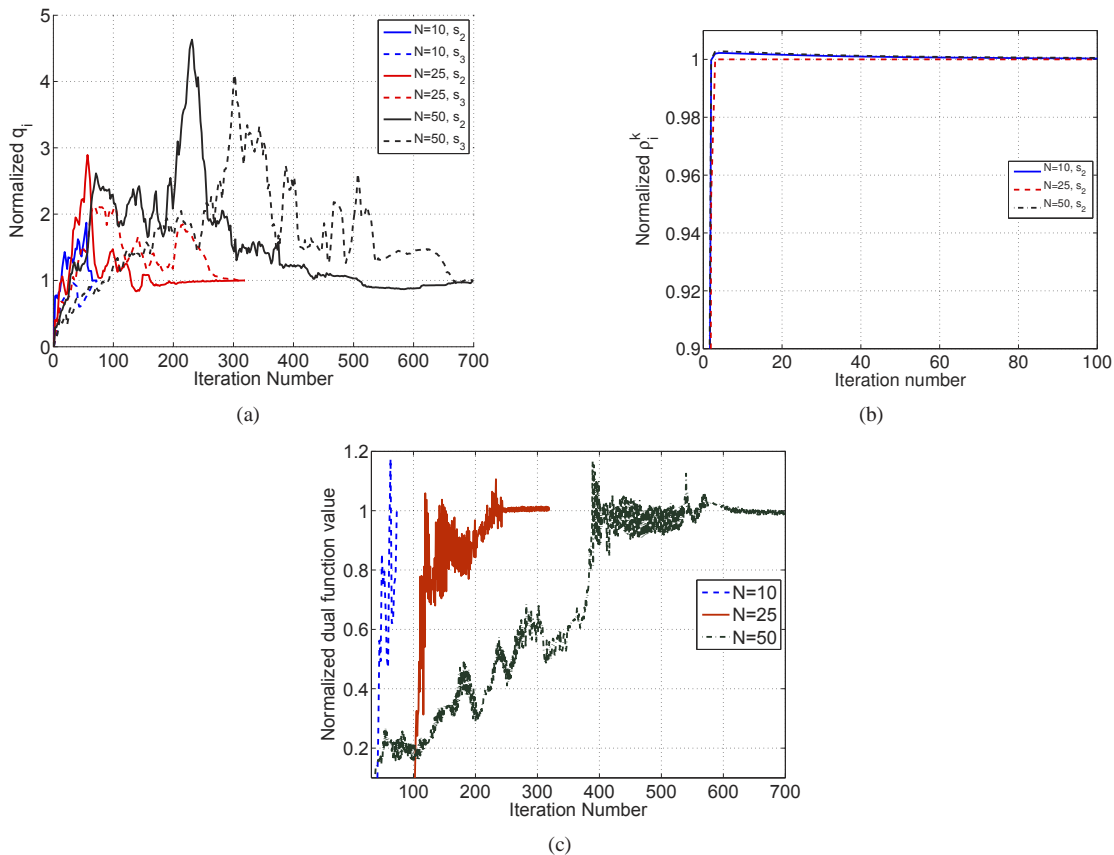


Fig. 9. Convergence of (a) q_i , (b) ρ_i^k , and (c) value of dual function in sample networks of sizes $N = 10, 25, 50$, and with $K = 2$. The values are normalized to their optimal value.

VI. CONCLUSIONS

In this paper, we have investigated the optimization of operational lifetime in event detection sensor networks using UWB communication. The specific sensor network task considered assumed sensing events with known locations under given detection requirements. We have assumed UWB signal properties and a simple MAC layer (no power control, random access), and we have considered variable generation bit rates at the sensors, which made it possible to tradeoff detection accuracy with energy consumption for transmission. Given this setup, we have formulated a convex optimization problem, which can be solved using standard methods at a central node, preferably the network sink. Moreover, we have provided a distributed method, which shares the computational load among the network nodes and requires mostly local communication among neighboring nodes. Numerical results show that our UWB-based maximum-lifetime joint event detection (UMLJE) approach and its distributed version are able to efficiently find the routes for maximum operational lifetime and achieve significant performance gains over previously proposed methods.

REFERENCES

- [1] I. F. Akyildiz, W. Su, Y. Sankarasubramaniam, and E. Cayirci, "Wireless sensor networks: a survey," *Computer Networks*, vol. 38, no. 4, pp. 393–422, 2002.
- [2] W. Ye, J. Heidemann, and D. Estrin, "Medium access control with coordinated adaptive sleeping for wireless sensor networks," *IEEE/ACM Transactions on Networking*, vol. 12, no. 3, pp. 493–506, June 2004.
- [3] D. Mirza, M. Owrang, and C. Schurgers, "Energy-efficient wakeup scheduling for maximizing lifetime of IEEE 802.15.4 networks," in *Proc. First International Conference on Wireless Internet*, Jul. 10–14, 2005, pp. 130–137.
- [4] Y. Xi and M. Yeh, "Node-based optimal power control, routing, and congestion control in wireless networks," *IEEE Trans. Inform. Theory*, vol. 54, no. 9, pp. 4081–4106, Sep. 2008.
- [5] C. Hua and T.-S. P. Yum, "Optimal routing and data aggregation for maximizing lifetime of wireless sensor networks," *IEEE/ACM Transactions on Networking*, vol. 16, no. 4, pp. 892–903, Aug. 2008.
- [6] Q. Dong, "Maximizing system lifetime in wireless sensor networks," in *Proc. Fourth International Symposium on Information Processing in Sensor Networks (IPSN)*, Apr. 15, 2005, pp. 13–19.
- [7] Y. Yang, R. S. Blum, and B. M. Sadler, "Energy-efficient routing for signal detection in wireless sensor networks," *IEEE Trans. Signal Processing*, vol. 57, no. 6, pp. 2050–2063, Jun. 2009.
- [8] J. Li and G. AlRegib, "Network lifetime maximization for estimation in multihop wireless sensor networks," *IEEE Trans. Signal Processing*, vol. 57, no. 7, pp. 2456–2466, Jul. 2009.
- [9] K. Lorincz, D. Malan, T. Fulford-Jones, A. Nawoj, A. Clavel, V. Shnyder, G. Mainland, M. Welsh, and S. Moulton, "Sensor networks for emergency response: challenges and opportunities," *Pervasive Computing, IEEE*, vol. 3, no. 4, pp. 16–23, Oct. 2004.
- [10] A. Mainwaring, D. Culler, J. Polastre, R. Szewczyk, and J. Anderson, "Wireless sensor networks for habitat monitoring," in *Proceedings of the 1st ACM international workshop on Wireless sensor networks and applications*, ser. WSN '02, 2002, pp. 88–97.
- [11] A. Milenkovic, C. Otto, and E. Jovanov, "Wireless sensor networks for personal health monitoring: Issues and an implementation," *Computer Communications*, vol. 29, no. 13-14, pp. 2521–2533, 2006.
- [12] H. Wang, N. Agoulmine, M. Ma, and Y. Jin, "Network lifetime optimization in wireless sensor networks," *IEEE Journal on Selected Areas in Communications*, vol. 28, no. 7, pp. 1127–1137, Sep. 2010.
- [13] J.-H. Chang and L. Tassiulas, "Maximum lifetime routing in wireless sensor networks," *IEEE/ACM Transactions on Networking*, vol. 12, no. 4, pp. 609–619, 2004.
- [14] R. Madan and S. Lall, "Distributed algorithms for maximum lifetime routing in wireless sensor networks," *IEEE Trans. Wireless Commun.*, vol. 5, no. 8, pp. 2185–2193, Aug. 2006.
- [15] A. Sankar and Z. Liu, "Maximum lifetime routing in wireless ad-hoc

- networks," in *Proc. of IEEE International Conference on Computer Communications (INFOCOMM)*, 2004.
- [16] J. Neyman and E. S. Pearson, "On the problem of the most efficient tests of statistical hypotheses," *Royal Society of London Philosophical Transactions Series A*, vol. 231, pp. 289–337, 1933.
- [17] H. V. Poor, *An introduction to signal detection and estimation (2nd ed.)*. New York, NY, USA: Springer-Verlag New York, Inc., 1994.
- [18] T. Q. S. Quek, M. Z. Win, and M. Chiani, "Distributed diversity in ultrawide bandwidth wireless sensor networks," in *Proc. Vehicular Technology Conference (VTC-Spring)*, vol. 2, May 30–Jun. 1, 2005, pp. 1355–1359.
- [19] I. Oppermann, L. Stoica, A. Rabbachin, Z. Shelby, and J. Haapola, "UWB wireless sensor networks: UWEN - a practical example," *IEEE Commun. Mag.*, vol. 42, no. 12, pp. S27–S32, Dec. 2004.
- [20] J. Zhang, P. Orlik, S. Z. A. Molisch, and P. Kinney, "UWB systems for wireless sensor networks," *Proc. IEEE*, vol. 97, no. 2, pp. 313–331, Feb. 2009.
- [21] F. Cuomo, C. Martello, A. Baiocchi, and F. Capriotti, "Radio resource sharing for ad hoc networking with UWB," *IEEE J. Select. Areas Commun.*, vol. 20, no. 9, pp. 1722–1732, Dec. 2002.
- [22] T. Melodia and I. F. Akyildiz, "Cross-layer QoS-aware communications for ultra wide band wireless multimedia sensor networks," *IEEE J. Select. Areas Commun.*, vol. 28, no. 5, pp. 653–663, Jun. 2010.
- [23] R. Merz, J. Widmer, J. Y. Le Boudec, and B. Radunovic, "A joint PHY/MAC architecture for low-radiated power TH-UWB wireless ad-hoc networks," *Journal of Wireless Communication and Mobile Computing*, vol. 5, no. 5, pp. 567–580, Jul. 2005.
- [24] H. Jiang and W. Zhuang, "Effective packet scheduling with fairness adaptation in Ultra-wideband wireless networks," *IEEE Trans. Wireless Commun.*, vol. 6, no. 2, pp. 680–690, Feb. 2007.
- [25] A. Rajeswaran, G. Kim, and R. Negi, "Joint power adaptation, scheduling, and routing for ultra wide band networks," *IEEE Trans. Wireless Commun.*, vol. 6, no. 5, pp. 1964–1972, May 2007.
- [26] K. Bai and C. Tepedelenlioglu, "Distributed detection in UWB wireless sensor networks," *IEEE Trans. Signal Processing*, vol. 58, no. 2, pp. 804–813, Feb. 2010.
- [27] J. Xu, Y. Hong, and L. Chen, "Bound on the operational lifetime of ultra wideband sensor network," in *Proc. of the First International Conference on Innovative Computing, Information and Control (ICICIC)*, 2006, pp. 80–84.
- [28] Y. Shi and Y. Thomas Hou, "On the capacity of UWB-based wireless sensor networks," *Comput. Netw.*, vol. 52, no. 14, pp. 2797–2804, 2008.
- [29] V. Shah-Mansouri and V. W. Wong, "Distributed maximum lifetime routing in wireless sensor networks based on regularization," in *IEEE Global Telecommunications Conference (GLOBECOM)*, Washington, DC, USA, Nov. 2007.
- [30] T. Banerjee, B. Xie, and D. P. Agrawal, "Fault tolerant multiple event detection in a wireless sensor network," *J. Parallel Distrib. Comput.*, vol. 68, pp. 1222–1234, September 2008.
- [31] J. Li and G. AlRegib, "Rate-constrained distributed estimation in wireless sensor networks," *IEEE Trans. Signal Processing*, vol. 55, no. 5, pp. 1634–1643, May 2007.
- [32] J.-J. Xiao, S. Cui, Z.-Q. Luo, and A. J. Goldsmith, "Power scheduling of universal decentralized estimation in sensor networks," *IEEE Trans. Signal Processing*, vol. 54, no. 2, pp. 413–422, Feb. 2006.
- [33] H. L. V. Trees, *Detection, Estimation, and Modulation Theory: Radar-Sonar Signal Processing and Gaussian Signals in Noise*. Melbourne, FL, USA: Krieger Publishing Co., Inc., 1992.
- [34] B. Radunovic and J. Y. Le Boudec, "Optimal power control, scheduling, and routing in UWB networks," *IEEE J. Select. Areas Commun.*, vol. 22, no. 7, pp. 1252–1270, Sep. 2004.
- [35] "IEEE standard part 15.4a: Wireless medium access control (MAC) and physical layer (PHY) specifications for low-rate wireless personal area networks (WPANs)," *IEEE Std 802.15.4a-2007 (Amendment to IEEE Std 802.15.4-2006)*, pp. 1–203, 2007.
- [36] A. F. Molisch, K. Balakrishnan, D. Cassioli, C. Chong, S. Emami, A. Fort, J. Karedal, J. Kunisch, H. Schantz, U. Schuster, and K. Siwiak, "IEEE 802.15.4a channel model-final report," IEEE 802.15.4a, Tech. Rep., 2005.
- [37] A. Krasnoperov, J.-J. Xiao, and Z.-Q. Luo, "Minimum energy decentralized estimation in a wireless sensor network with correlated sensor noises," *EURASIP J. Wirel. Commun. Netw.*, vol. 2005, no. 4, pp. 473–482, 2005.
- [38] L. Xiao, M. Johansson, and S. Boyd, "Simultaneous routing and resource allocation via dual decomposition," *IEEE Trans. Commun.*, vol. 52, no. 7, pp. 1136–1144, Jul. 2004.
- [39] S. Boyd and L. Vandenberghe, *Convex Optimization*, 4th ed. Cambridge University Press, 2004.
- [40] J. Ryckaert et al., "A CMOS Ultra-Wideband Receiver for Low Data-Rate Communication," *IEEE J. Solid-State Circuits*, vol. 42, no. 11, pp. 2515–2527, Nov. 2007.



Ghasem Naddafzadeh Shirazi (S'08) received his B.Sc. degree in Computer Science & Engineering (CSE) as the top rank student from Shiraz University, Iran (2006), and his Masters degree in Electrical & Computer Engineering (ECE) from National University of Singapore (2009). During his Masters study, he was affiliated with the Institute for Infocomm Research (I²R), Singapore, and won the Best Student Paper Award at the IEEE International Conference on Ultra-Wideband (ICUWB'08) for analyzing cooperative MAC protocols for UWB

communication.

He is currently a PhD candidate at the ECE Department, University of British Columbia, Canada. He has served as a technical program assistant and session chair in IEEE Vehicular Technology Conference (VTC'08, Singapore), and IEEE ICUWB'09 (Vancouver). His research interests include optimization in wireless sensor networks, UWB (cooperative) communication, and applications of machine learning in wireless networks.



Lutz Lampe (M'02, SM'08) received the Diplom (Univ.) and the Ph.D. degrees in electrical engineering from the University of Erlangen, Germany, in 1998 and 2002, respectively. Since 2003 he has been with the Department of Electrical and Computer Engineering at the University of British Columbia, where he is a Full Professor.

He is (co-)recipient of a number of Best Paper Awards, including awards at the 2006 IEEE International Conference on Ultra-Wideband (ICUWB), 2010 IEEE International Conference on Communications (ICC), and 2011 IEEE International Conference on Power Line Communications (ISPLC). He was awarded the UBC Killam Research Prize in 2008, the Friedrich Wilhelm Bessel Research Award by the Alexander von Humboldt Foundation in 2009, and the UBC Charles A. McDowell Award of Excellence in Research in 2010.

Lutz Lampe is an Editor for the IEEE Transactions on Wireless Communications and the IEEE Communications Surveys and Tutorials, and he has served as Associate Editor for the IEEE Transactions on Vehicular Technology from 2004 to 2008 and the International Journal on Electronics and Communications (AEUE) from 2007 to 2011. He was General Chair of the 2005 International Symposium on Power Line Communications (ISPLC) and the 2009 IEEE International Conference on Ultra-Wideband (ICUWB). He is Chair of the IEEE Communications Society Technical Committee on Power Line Communication.